DMD Fast Forward. Published on September 22, 2009 as doi:10.1124/dmd.108.025494

DMD 25494

Prediction of Human Drug and Drug Interactions from Time-Dependent Inactivation of CYP3A4 in Primary Hepatocytes Using a Population-Based Simulator

Lilly Xu, Yuping Chen, Yvonne Pan, Gary L. Skiles, and Magang Shou

Department of Pharmacokinetics and Drug Metabolism, Amgen Inc., One Amgen Center Drive, Thousand Oaks, CA 91320, USA

DMD Fast Forward. Published on September 22, 2009 as DOI: 10.1124/dmd.108.025494
This article has not been copyedited and formatted. The final version may differ from this version.

Running Title: Prediction of Human Drug Drug Interactions from CYP inhibition

* **Address to correspondence to:** Dr. Magang Shou, Department of Pharmacokinetics and Drug Metabolism, 30E-2-B, Amgen, One Amgen Center Drive, Thousand Oaks, CA91320-1799; Tel: (805) 447-4247; Fax: (805) 375-9515; E-mail: mshou@amgen.com

No. of Text Pages: 16
No. of Tables: 5
No. of Figures: 5
No. of References: 66
No. of Words in Abstract: 265
Introduction: 662
Discussion: 1293

The Abbreviations used: TDI, time-dependent inactivation; IVIVE, in vitro in vivo extrapolation; IVIVC, in vitro in vivo correlation; HLM, human liver microsomes; $f_{u,p}$, unbound fraction in plasma; $f_{u,\ mics}$, unbound fraction in HLM; $f_{u,\ hept}$, unbound fraction in hepatocytes; KHB, Krebs-Henseleit Buffer; K_a, absorption rate constant; DME, drug metabolizing enzyme; k_{inact}, maximum inactivation rate constant; K_I, inhibitor concentration leading to 50% of k_{inact}; k_{deg}, rate constant for enzyme degradation; CLA, clarithromycin, DIL, diltiazem, ERY, erythromycin, VER, verapamil; TAO, troleandomycin; ABT, 1-aminobenzotriazole; MDZ, midazolam; 1-OH MDZ, 1-hydroxy midazolam; $f_{m,\ CYP}$, fraction of a drug cleared by a CYP; $CL_{int,\ E}$, intrinsic clearance for enzyme inactivation; RSS, Residual Sum of Squares; K_a, absorption rate constant.

Abstract

Time-dependent inactivation (TDI) of human cytochromes P450 3A4 (CYP3A4) is a major cause of clinical drug drug interactions (DDIs). Human liver microsomes (HLM) are commonly used as an enzyme source for evaluating the inhibition of CYP3A4 by new chemical entities (NCEs). The inhibition data can be then extrapolated to assess the risk of human DDIs. Using this approach, under- and over-predictions of in vivo DDIs have been observed. In the present study, human hepatocytes were used as an alternative to HLM. Hepatocytes incorporate the effects of other mechanisms of drug metabolism and disposition (i.e. phase II enzymes and transporters) that may modulate the effects of TDI on clinical DDIs. The in vitro potency (K_I and k_{inact}) of five known CYP3A4 TDI drugs (clarithromycin, diltiazem, erythromycin, verapamil and troleandomycin) was determined in HLM (pooled, n=20) and hepatocytes from two donors (D1 and D2) and the results were extrapolated to predict in vivo DDIs using a SimCYP population trial-based simulator. In comparison to observed DDIs, the predictions derived from HLM appeared to be over-estimated. The predictions based on TDI measured in hepatocytes were better correlated with the DDIs (n = 37) observed in vivo (R^2 = 0.601, D1 and 0.740, D2) than those from HLM (R^2 = 0.451). In addition, using hepatocytes a greater proportion of the predictions were within a 2-fold range of the clinical DDIs compared to using HLM. These results suggest that DDI predictions from CYP3A4 TDI kinetics in hepatocytes could provide an alternative approach to balance HLM-based predictions that can sometimes substantially over-estimate DDIs and possibly lead to erroneous conclusions about clinical risks.

Introduction

Clinical drug-drug interactions (DDIs) are a major source of adverse drug reactions (ADR) and are becoming a growing problem with multiple-drug therapy. The most common DDIs are caused by inhibition of enzymes responsible for drug clearance and result in increased bioavailability, systemic exposure, and half life of a victim drug (Obach, 2003;Gomez, et al., 1995;Greenblatt, et al., 1998b). The resulting increased exposure to the affected drug can lead to enhancement of the pharmacodynamic (PD) effects or serious side effects in humans. DDIs not only affect patient safety but also add to the cost of drug development because of the high costs of failure in clinical development. These issues have prompted the search for approaches to predict the potential for DDIs at the earliest possible stages of drug development (Ito, et al., 1998;von Moltke, et al., 1998; Obach, et al., 2007; Obach, et al., 2005; Mayhew, et al., 2000). Information about the inhibition of drug-metabolizing enzymes (DMEs) obtained using in vitro systems can provide a basis for predicting DDIs in man and thereby facilitate decisions about advancement of drug candidates and aid in planning of clinical DDI studies.

Human 3A4 is the most abundant cytochromes P450 (CYP) isozyme and is responsible for the metabolism of approximately 50% of all drugs (Guengerich, 2003). The substrates of CYP3A4 are chemically diverse, and this broad substrate specificity renders CYP3A4 susceptible to reversible or irreversible inhibition by a variety of drugs. Irreversible, time-dependent inactivation (TDI) or mechanism-based inhibition (MBI) of CYP3A4 refers to inactivation of the enzyme via formation of metabolic intermediates that bind tightly and irreversibly to the CYP3A4 enzyme in a time- and concentration-dependent manner. Two kinetic parameters, k_{inact} (maximum inactivation rate constant) and K_I (inhibitor concentration leading to 50% of k_{inact}) that describe the potency of the TDI are commonly used in the prediction of potential clinical DDIs. These TDI parameters are most commonly determined using human liver microsomes (HLM). It has, however, been our observation that for some drugs the DDIs predicted by this method are far greater than any DDI that occurs clinically, even for highly potent inhibitors

(unpublished observation). This suggests that in some instances microsomal incubations are inadequate to properly account for all of the factors that ultimately determine the extent of clinical DDIs.

Human hepatocytes have been widely used in drug discovery and development to measure intrinsic metabolic clearance and to measure the potential for a drug to cause DDIs due to either inhibition or induction of CYP enzymes. Because hepatocytes are an intact cellular system, not only is their CYP activity preserved, but other microsomal enzymes that require co-factors and non-microsomal DMEs are also active. In addition, the effects of passive and active uptake and efflux on intracellular concentrations of a drug are also maintained in hepatocytes. This is important because inhibitory responses of a drug will depend on the intracellular concentration in hepatocytes, which for some drugs could be substantially different than the concentrations that occur extracellularly or in microsomes. In this study, in vitro TDI kinetic parameters of five known CYP3A4 inhibitors were measured in HLM and hepatocytes. The kinetic parameters derived from these studies were used for in vitro in vivo extrapolations (IVIVE) of clinical DDIs using SimCYP. SimCYP is a population-based clinical trial simulator that is increasingly being used for pharmacokinetic (PK) and DDI predictions. SimCYP incorporates information on properties of absorption, distribution, metabolism, elimination and pharmacokinetics in population and provide mean (or median) values with extremes of both PK and DDIs that may occur in the population (Rostami-Hodjegan and Tucker, 2007). In the present study SimCYP was used to predict clinical DDIs from the in vitro TDI kinetic parameters of five CYP3A4 inhibitors measured in HLM and human hepatocytes (two donors), and the predictions were then compared to clinically observed DDIs. The study was conducted to better understand whether in vitro TDI data generated in human hepatocytes can be utilized to more reliably assess the risk of DDIs for compounds in preclinical development.

Materials and Methods

Materials. Cryopreserved human hepatocytes were obtained from two hepatic donors. Donor 1 (D1) was obtained from a female Caucasian donor aged 52 years (Lot number = HH230, In Vitro Technologies Corp., Baltimore, MA). Donor 2 (D2) was a pool of hepatocytes from three individuals, one female aged 20 years, and two males at ages 42 and 81 years, respectively (Invitrogen-CellzDirect, Durham, NC). Enzymatic activity of the individual CYPs in the hepatocytes were well characterized by the vendors. Pooled HLM (n =20 donors, 10 from each gender) were purchased from XenoTech Corp. (Kansas, KS). Clarithromycin (CLA), diltiazem (DIL), erythromycin (ERY), verapamil (VER), troleandomycin (TAO), 1-aminobenzotriazole (ABT) and Krebs-Henselit Buffer (KHB) were purchased from Sigma-Aldrich Co. (St Louis, MO). Midazolam (MDZ) and 1-hydroxy midazolam (1-OH MDZ) were purchased from BD Gentest Co. (Bedford, MA).

Time-Dependent Inactivation of CYP3A4. Each inhibitor was pre-incubated at varying concentrations (5 concentrations) at 37ºC in an incubation mixture (0.2 mL) containing 1 mg/mL HLM, 1 mM NADPH and 0.1 M phosphate buffer (pH = 7.4). The pre-incubation times at each inhibitor concentration were 0, 10, 20, 30, and 45 min. After the pre-incubation, an aliquot (10 µL) was transferred to a reaction mixture (190 µL, 20-fold dilution) containing 1 mM NADPH and 20 µM MDZ in 67 mM phosphate buffer. The reaction was incubated for an additional 5 min and terminated by the addition of 200 µL acetonitrile containing 0.05% formic acid and internal standard (terfenadine; 0.5 µM final conc.). The sample was then centrifuged and the supernatant was analyzed by LC-MS to measure remaining CYP3A4 activity (MDZ 1-hydroxylation).

Cryopreserved human hepatocytes from the two donors were thawed at 37°C and washed twice with KHB. The hepatocytes were placed in a 37°C incubator (Steri-Cult CO_2 Incubator, Model 3310, Thermo Electron Corporation, Waltham, MA) under an atmosphere of 95% air / 5% CO_2 and 90% relative humidity. The individual inhibitors were pre-incubated in the hepatocyte suspensions in triplicate (1 mL incubation, 1 x 10^6

cells/mL). 200 µL aliquot from each cell suspension was taken at 0, 5, 10, and 15 min, respectively for CYP3A4 activity measurement. Each aliquot of cells was washed and centrifuged (500g, 10 min) and the cell pellets were re-suspended with 200 µL KHB containing 20 µM MDZ. The reactions proceeded at 37°C for 10 min and were quenched with acetonitrile (2 volumes) containing an internal standard (terfenadine; 0.5 µM final conc.). The samples were centrifuged and the supernatants were analyzed by LC-MS/MS (described below) to measure disappearance of MDZ and formation of the metabolite 1-OH-MDZ (Fig. 1).

Measurement of Free Drug Concentrations in In Vitro Incubations and Plasma. Unbound fractions of the inhibitors in human hepatocytes were measured by two methods (treatment with alamethicin and ABT). Alamethicin is known to cause cells to become permeable to low molecular weight molecules, such as NADPH, resulting in ablation of metabolic capability (Matic, et al., 2005). Human hepatocytes were incubated with 25-50 µM alamethicin in KHB in a 37°C incubator for 30 min. Under these conditions, the cells (10^6 cells/mL) remained intact but the cell viability was <10% monitored by dye exclusion analysis (trypan blue) and their ability to metabolize the inhibitors was minimized. The suspended cells were incubated for 15 min at 37^oC in a water bath with the inhibitors at concentrations approaching their K_I and then centrifuged at 500 g for 10 min. 100 µL aliquot of the supernatants (unbound concentration) were analyzed by LC/MS. The total concentration was measured by quenching the cell suspensions (100 µL aliquot each) containing the inhibitor with acetonitrile (2 volumes) before centrifugation. Similarly, the unbound fractions in hepatocytes in the absence and presence of ABT (a mechanism-based inhibitor of multiple CYPs) were also measured (Austin, et al., 2005). Human hepatocytes were treated with 1 mM ABT dissolved in DMSO and pre-incubated in the presence of 1 mM NADPH in a water bath at 37^oC for 60 min, and then centrifuged (500g, 10 min) to remove the remaining ABT. The cell pellets were re-suspended with buffer and incubated for an additional 15 min after adding the individual inhibitors. 100 µL aliquot of the supernatants (unbound concentration) from centrifuge was analyzed by LC/MS. Cells incubated in the absence of alamethicin

DMD Fast Forward. Published on September 22, 2009 as DOI: 10.1124/dmd.108.025494
This article has not been copyedited and formatted. The final version may differ from this version.

or ABT served as a control. In each case the unbound fraction ($f_{u, hept}$) was calculated as the ratio of unbound to total concentration.

For measurement of unbound fractions in human plasma and HLM, frozen human plasma or HLM was thawed and preheated at 37°C. The plasma (2 mL) or HLM (1 mg/mL, 2 mL) in polypropylene centrifuge tubes (Corning Inc., NY) was incubated for 15 min with the individual inhibitors at the same concentrations tested in hepatocytes. After the incubation period, aliquots (800 µL, n = 2) were transferred to pollyallomar tubes (Beckman Coulter, Inc., Fullerton, CA) for ultra-centrifugation. The ultra-centrifugation was performed for 3 hr at 37°C and 627,000 g using an MLA-130 rotor and an Optima™ Max Ultracentrifuge (Beckman Instruments, Palo Alto, CA). Supernatant (50 µL) from each sample was mixed with 200 µL of acetonitrile containing an internal standard (proprietary Amgen compound, 0.125 µg/mL). The samples were then centrifuged for 10 min at 405 x g, and then 200 µL of supernatant was transferred into a 96-well plate and dried under a nitrogen stream. The samples were reconstituted with 50% MeOH/H_2O (100 µL) and analyzed by LC-MS/MS. Standard curves were generated by a sequential dilution of the analyte and quantified by the peak area ratio of analyte to internal standard added. Concentrations of the analytes were determined by the standard curves generated in the same matrix. The unbound fraction in plasma ($f_{u,p}$) was calculated as the ratio of the concentration measured in the ultracentrifugation supernatant to the concentration measured without the ultracentrifugation. Drug recovery values were also calculated by a ratio of the drug concentration in the plasma, HLM or hepatocyte sample measured to total concentration added. All the LC-MS/MS analyses were performed in triplicate. The unbound fractions of the five inhibitors measured in plasma, HLM and hepatocytes are listed in Table 1.

Measurement of Metabolite by LC-MS/MS. The reaction samples (20 µL) obtained from the TDI experiments in HLM and hepatocytes were injected into a LC-MS/MS equipped with a reversed phase column (Sprite Armor C18 2.0 x 30 mm (10 µm) column), Shimadzu SCL-10AVP pumps, a Leap HTCPAL auto-sampler, and a Sciex API 3000 mass spectrometer. Analytes were eluted with a mobile phase (A: 0.1% formic acid in water and B: 0.1% formic acid in acetonitrile) at a flow rate of 0.3 mL/min. A gradient

DMD Fast Forward. Published on September 22, 2009 as DOI: 10.1124/dmd.108.025494
This article has not been copyedited and formatted. The final version may differ from this version.

elution started at 95% A (0.3 min) then ramped to 5% A (0.4 min) and was held at 5% A for 0.5 min before return to the initial condition. The metabolite, 1-OH MDZ (transition 342.1/324.3), was detected in the positive ion mode by Selective Reaction Monitoring. The peak area of the analyte was expressed as a ratio of the internal standard (terfenadine, mass transition 472.3/436.2). The concentrations of metabolite formed during the incubations were interpolated from the calibration curve.

Data Analysis. Fractions of CYP3A4 activity remaining ($[E]/[E]_{tot}$) in the presence of an inhibitor ([I]) after a pre-incubation time (t) are described by Eqn. 1, where the rate of inactivation (k_{obs}) is the slope of the natural log of the percent enzyme activity ($\ln [E]/[E]_{total}$) vs. pre-incubation time (Eqn. 2). K_I and k_{inact} were determined by non-linear fitting of Eqn. 2 to the observed k_{obs} in HLM and hepatocytes (Fig. 1) using SigmaPlot 10.0 (Systat Software, Inc., Chicago, IL). k_{inact} and K_I were the maximal velocity of inactivation (k_{inact}) and the inhibitor concentration that yields a half of k_{inact}, respectively.

$$Ln\frac{[E]}{[E]_{tot}} = \frac{-k_{inact}\cdot[I]\cdot t}{K_I + [I]} \qquad (1)$$

$$k_{obs} = \frac{k_{inact}\cdot[I]}{K_I + [I]} \qquad (2)$$

The average (n = 3) remaining enzyme activity (%) measured as MDZ 1-hydroxylation formation was expressed as a percentage of the time-matched control samples without inhibitor. The initial slope (k_{obs}) of each inactivation curve and its variance were determined by regression analysis using Sigma Plot. The kinetic parameters k_{inact} and K_I were obtained from a non-linear fitting of k_{obs} against the inhibitor concentration ([I]) using Eqn. 2. The correlation analyses between predicted and clinical DDIs were performed by linear regression with ANOVA. R^2 (correlation coefficient) and RSS (Residual Sum of Squares, a measure of the size of the residuals,

which are the differences of the actual data points from regression modeled values) were also determined.

SimCYP Simulator for Human DDI Prediction. DDI simulations were performed using SimCYP® population-based ADME simulator (Version 7.11). The physiologically-based model and the differential equations used by the simulator have been described (Yang, et al., 2006). In vitro K_{inact} and K_I are incorporated into the model for simulating the level of CYP3A4 inhibition (Yang, et al., 2006; Ito, et al., 2003). In addition, experimentally determined or published V_{max} and K_m values (or intrinsic clearance) and unbound fractions (f_u) of the test substrates being modeled are used in the simulation. The simulator uses these data for all CYPs that collectively contribute to the clearance of a particular substrate; consequently, the individual contribution of CYP3A4 ($f_{m,CYP3A4}$) to the total metabolic clearance of each substrate can be determined as shown in Table 2. This allows DDI simulations with substrates that are known to be poorly metabolized by CYP3A4 such as those tested here (theophylline, metoprolol, and imipramine). The model assumes first-order oral absorption, single-compartment distribution, and elimination by renal excretion and hepatic metabolism. The simulator also integrates a gut model since substantial levels of CYP3A4 are also expressed in that tissue and can contribute to the overall metabolism of a drug (Yang, et al., 2007, 2008).

The time-based simulations are performed according to the trial design (Einolf, 2007;Rostami-Hodjegan and Tucker, 2007). Virtual populations were generated within SimCYP using reported information on genetic (i.e. CYP genetic polymorphism and abundance in liver and gut), physiological and demographic variability relevant to the appropriate clinical DDI studies. PK parameters (CL, V_{dss}, K_a, gut absorption and hepatic metabolism etc.) for the inhibitors and victim drugs as well as other associated ADME properties such as in vitro turnover (K_m and V_{max} for the substrates) are incorporated in the SimCYP library. The mean CYP3A4 abundance of the population in liver (137 pmol/mg liver protein) and gut (66.2 nmol/total gut, predicted DDIs associated with gut CYP3A4 inhibition is also included) were used. The PK parameters of the five inhibitors for simulation of plasma concentration profiles are listed in Table 3. In vitro data

measured such as fractions unbound (plasma, HLM and hepatocytes), kinetic constants (K_I and k_{inact}) and PK parameters for the inhibitors were entered into SimCYP for the predictions. Dose, dose interval, and the duration of administration of the inhibitors and victim drugs were set according to the regimens of the clinical DDI trials described in the literature reports. The trials were designed and performed using a virtual population of healthy volunteers in 10 trials of 10 subjects, each aged 18-65 years with a ratio of 0.34, female: male). A half life of 48 hours for CYP3A4 degradation (k_{deg} = 0.0144 hr^{-1}) was used for the CYP3A4 clearance for inactivation. The DDIs were determined as the fold increase in AUC of the victim drugs in the presence versus the absence of the inhibitors. The median and population extremes (5^{th} and 95^{th} percentiles) were determined.

Analysis of Variance (ANOVA). The variability of the dependent variable was analyzed by ANOVA (root mean residual sum of square, RMRSS and mean residual sum, MRS) using Eqns. 3 and 4, where y_i = predicted value, x_i = observed clinical value and i = 1,2,3,…n. An RMRSS value that approaches zero indicates the least variability between predicted and observed DDIs, and the MRS value indicates the subsequent bias. A negative bias in MRS indicates under-prediction while a positive bias indicates over-prediction.

$$RMRSS = \sqrt{\frac{1}{n}\sum_{1}^{n}(y_i - x_i)^2} \qquad (3)$$

$$MRS = \frac{1}{n}\sum_{1}^{n}(y_i - x_i) \qquad (4)$$

Results

Unbound Fractions in HLM and Hepatocytes. The unbound fractions of the inhibitors in plasma ($f_{u,p}$), HLM ($f_{u,mics}$), and hepatocytes ($f_{u,hept}$) are shown in Table 1. The unbound fractions among the inhibitors varied widely, from 0.015 (TAO) to 0.326 (ERY) in plasma, from 0.154 (TAO) to 0.870 (ERY) in HLM, and from 0.715 (TAO) to 0.980 (CLA) in hepatocytes. When determining the unbound fractions in hepatocytes, metabolism of the drug can confound the measurement. Accordingly, hepatocytes were pre-incubated with alamethicin (50 μM) or ABT (1 mM) to minimize metabolism of the inhibitors. Alamethicin permeabilizes cells via pore formation resulting in leakage of intracellular NADPH required for NADPH-dependent metabolism. We have demonstrated that under these experimental conditions, alamethicin inhibited testosterone 6β-hydroxylation in primary hepatocytes by 78% (unpublished data). This approach does not, however, correct for the effects of active uptake or efflux transport. It may affect or negate active transport of drugs. ABT is a mechanism-based inhibitor of multiple CYPs. The free concentrations of DIL, ERY and VER measured in the untreated cells were lower than when cells were pre-treated with either alamethicin or ABT (Table 1). The unbound fractions determined with ABT were slightly lower than that with alamethicin, but they were still quite similar; therefore, the values measured from the cells treated with alamethicin were used for all DDI predictions.

Time-Dependent Inactivation of CYP3A4 Activity. CLA, DIL, ERY, VER and TAO have been previously reported as time-dependent CYP3A4 inhibitors both in microsomes and in vivo. Little is known, however, about their TDI in human hepatocytes. When pre-incubated with HLM and hepatocytes, each compound was shown to be capable of inhibiting MDZ 1-hydroxylation in a time- and concentration-dependent manner. The slopes (k_{obs}) of remaining enzyme activity (log scale) vs. pre-incubation time at various concentrations of a given inhibitor were generated and maximal rates of inactivation (k_{inact}) and apparent K_I constants of the inhibitors were determined from the non-linear fitting of Eqn. 2 to the observed data (k_{obs} vs. [I]) (Fig. 2 and Table 4). K_I values were also corrected by the unbound fractions for a comparison between HLM and

DMD Fast Forward. Published on September 22, 2009 as DOI: 10.1124/dmd.108.025494
This article has not been copyedited and formatted. The final version may differ from this version.

hepatocytes (Table 4). In most circumstances, values for unbound K_I in HLM were smaller than those in hepatocytes from both donors.

The overall potency of a time-dependent inhibitor can be described as the intrinsic clearance of enzyme via inactivation [$CL_{int,E} = k_{inact}/(K_I \cdot f_u)$]. Using this method the inhibitor potencies were ranked as TAO (2.22) >> DIL (0.035) > VER (0.026) > CLA (0.012) ≅ ERY (0.012) in HLM, and as TAO (0.13, 0.05) > VER (0.011, 0.008) > DIL (0.009, 0.004) > CLA (0.005, 0.002) > ERY (0.001, 0.001) in hepatocytes from the two donors, respectively. The inhibitors were shown to be 2 (VER) – 44 (TAO)-fold more potent in HLM than that in hepatocytes. Of all the inhibitors, TAO was the most capable of inactivating CYP3A4-mediated MDZ 1-hydroxylation activity with a low K_I (0.19-1.05 μM) and high k_{inact} (0.038-0.065 min^{-1}) in both HLM and hepatocyes, respectively.

In Vivo Drug Drug Interactions. In order to assess the reliability of the vitro in vivo correlations (IVIVC), clinically observed DDIs reported in the literature were collected. A total of 37 pairs of inhibitor-substrate interactions were used in the correlation analysis (Table 5). In these cited clinical studies the doses, dose regimens, and duration of inhibitor and substrate administration were provided. These study designs were identically used for the SimCYP predictions. In addition, the predicted $[I]_{max,\ ss}$ of the inhibitors at the given dose regimens (maximum plasma concentrations of the individual inhibitors at steady state) were simulated (Table 5). A SimCYP simulated plasma concentration-time profile of CLA at a given dose (500 mg, BID for 9 days) as an example is shown in Fig. 3a. The $C_{max,\ ss}$ values of all inhibitors were generally in agreement with the in vivo concentrations reported in literature which fall within two-fold or less (Table 3).

Simulation of DDIs from In Vitro Data. The in vitro TDI kinetic parameters (K_I and k_{inact}) and protein binding data of the inhibitors in plasma, HLM, and hepatocytes were employed to predict in vivo DDIs in SimCYP simulations. The degradation rate of CYP3A4 used for the simulation was selected (k_{deg} for CYP3A4 = 0.0144 $hour^{-1}$, equivalent to a half-life of 48 hours). As seen in Table 5, the majority of the victim drugs

used in this investigation is the known substrates of CYP3A4 (i.e. alprazolam, simvastatin, triazolam, sildenafil, cyclosporine, and MDZ). In addition, some of the drugs are also metabolized by other CYPs (i.e. imipramine, metroprolol, omeprazole, and theophylline). K_m and V_{max} of the victim drugs for individual CYPs were entered in SimCYP to identify contribution of CYP3A4 to total clearance of the drugs ($f_{m,CYP}$) (Table 2). Clearly, the $f_{m,CYP3A4}$ values of the poor substrates for CYP3A4 are low. Input concentrations in the gut and hepatic portal vein were also estimated using SimCYP (data not shown).

The simulated plasma concentration-time profile of a drug (simvastatin) in the presence and absence of a given inhibitor (CLA) is shown in Fig. 3b. Exposure of simvastatin is markedly increased due to the inhibition of CYP3A4 by CLA resulting in the profound decrease in intrinsic clearance in both liver and gut as a function of time depicted in Figs. 3C and D. The DDIs predicted from the in vitro data in HLM and hepatocytes (D1 and D2) are listed in Table 5. The median values and the 5^{th} and 95^{th} percentiles in the population (10 trials) are shown. The predicted in vivo DDIs (n = 37) from TDI of the five inhibitors between the two hepatocyte donors (D1 and D2) were reasonably well correlated ($R^2 = 0.747$) (Fig. 4C). The TDI values predicted from D1 and D2 were slightly different as should be expected from heterogeneity among human donors. The correlations of predicted DDIs between HLM and hepatocytes from each donor were 0.813 (D1) and 0.549 (D2), respectively (Figs. 4A and B).

Fig. 5 shows the correlations of 37 pairs of substrate-inhibitor interactions between predicted and observed DDIs. Three correlation analyses of the predictions (HLM, D1 and D2) with the in vivo observations were performed (Figs. 5A, C and E). Predictions based on the two hepatocyte donors ($R^2 = 0.601$, D1 and $R^2 = 0.740$, D2) (Figs. 5C and E) were better correlated than than those based on HLM ($R^2 = 0.451$) (Fig. 5A). In addition, the majority of the DDIs (35 and 30 out of 37 DDI pairs for D1 and D2, respectively) predicted from hepatocyte data were within 2-fold of the actual clinical DDIs. In comparison, 27 out of 37 DDI pairs from HLM were within a 2-fold range. Most of the HLM outliers were ERY based DDIs (Fig. 5B). Additionally, 24 out of 37 of

the HLM-based predictions over-estimated the DDIs actually observed. The DDIs based on hepatocytes from D1 were uniformly distributed about unity (19:18) (Fig. 5D). In contrast, 35 of 37 DDIs predictions based on hepatocytes from D2 under-predicted DDIs observed in the clinic. In the ANOVA analyses, the RMRSS values for the predictions from D1 and D2 were smaller (1.25 and 1.63) than those from HLM (3.95), indicating a small degree of variability between the predicted and observed values. In addition, the positive mean residual sum (MRS) in the predictions from HLM (1.87) is consistent with an over-prediction of the results. Conversely, the negative MRS value from D2 (-1.17) indicates a bias for under-prediction of the data. The predictions from D1 had no significant bias with a MRS of 0.25.

Discussion

In vitro approaches are being increasingly used to predict clinical DDI risks associated with NCEs (Ito, et al., 1998; Obach, et al., 2005;Obach, et al., 2007;Mayhew, et al., 2000). Successful predictions can result in decreased compound attrition during drug development, and can reduce the costs and time associated with failed clinical trials. TDI of CYP3A4 has been reported to be a major cause of clinical DDIs. Due to the primary role of CYP3A4 in drug disposition there is a need for better tools to effectively predict the potential for clinical DDI from in vitro data when the inhibition is mechanism-based. The present study provides an initial demonstration of the potential utility of hepatocytes to empirically account for the various factors that affect a reliable in vitro assessment of TDIs, and to assess potential clinical DDIs using a SimCYP-directed IVIVE.

The capability of CLA, DIL, ERY, VER and TAO to inactivate CYP3A4 activity in HLM and hepatocytes was confirmed. The kinetic parameters of CYP3A4 inactivation (K_I and k_{inact}) by the five inhibitors in HLM have been previously characterized (Atkinson, et al., 2005;Mayhew, et al., 2000;Polasek, et al., 2004;Yeo and Yeo, 2001). The findings in the current study were consistent with those previously reported parameters (see the values in the footnote of Table 4). Hepatocytes were also used to determine estimates of the TDI kinetic parameters for comparison with HLM. While cryopreserved hepatocytes were used, activities of the major CYPs in these hepatocytes were well characterized by the vender. The inactivation of CYP3A4 in hepatocytes was observed to exhibit the typical characteristics of concentration- and pre-incubation time-dependence. The TDI caused by the five inhibitors and measured as enzyme inactivation ($CL_{int,\ E}$) was found to be 2 to 44-fold greater in HLM than in hepatocytes. Such differences can of course impact the accuracy of any in vivo DDI predictions. CLA, DIL, ERY, and TAO have been shown to be selective mechanism-based inhibitors of CYP3A4 so the predicted in vivo DDIs are largely due to the TDI of CYP3A4. VER, however, was shown to inhibit not only CYP3A4 but also competitively inhibit CYP2C9, CYP2C19

DMD Fast Forward. Published on September 22, 2009 as DOI: 10.1124/dmd.108.025494
This article has not been copyedited and formatted. The final version may differ from this version.

and CYP2D6. Its IC_{50} or K_i values in pooled HLM were reported to be 118 μM for the CYP2C9-catalyzed formation of 4-OH tolbutamide (Wester, et al., 2000), 43.8 μM for the CYP2C19-catalyzed formation of 4-OH mephenytoin (Foti and Wahlstrom, 2008), and 30.4 μM for the CYP2D6-catalyzed formation of O-desmethylmetoprolol (Kim, et al., 1993). As shown in Table 5, predictions of VER-depedent DDIs with the test substrates metoprolol, imipramine and theophylline that are metabolized by CYPs other than CYP3A4 were apparently underestimated.

As shown by the correlation analyses in Fig. 5, DDIs predicted from TDI parameters measured in HLM were generally greater than those predicted from hepatocytes, due largely to lower K_I values measured in vitro. These apparent differences in the TDI parameters measured between the two preparations can probably attributed to difference in the actual concentrations of the inhibitors available to the target enzyme; that is, intracellular concentrations of the inhibitors were different from the nominal or extra-cellular concentrations used for calculation of the kinetic parameters. Factors that may cause this difference include rapid metabolism, and active uptake or efflux of the inhibitors by transporters. For example, VER (Crivellato, et al., 2002), DIL (Saeki, et al., 1993) and ERY (Takano, et al., 1998) are known to be either substrates for or inhibitors of MDR1 and/or MRPs in human. In addition, it has been reported that VER (Tracy, et al., 1999), DIL (Sutton, et al., 1997), ERY (Wang, et al., 1997b), and CLA (Rodrigues, et al., 1997) were metabolized by CYP3A4 and other CYPs. Uptake, efflux, or rapid metabolism of the inhibitors can alter the equilibrium between the intra- and extracellular concentrations, which affects the apparent K_I and leads to differences in the predictions.

The unbound fractions of the inhibitors in plasma were used in the predictions in adherence to the principle that under conditions of rapid equilibrium only free drug is available for metabolism or enzyme inhibition. Corrections in SimCYP were also made for the substantial differences in drug concentration in systemic circulation, the hepatic portal vein, and in the gut. These corrections help prevent under-estimations of DDIs that can result from using only systemic blood concentrations for the predictions (Ito, et al.,

1998). The effect of the inhibitors on first pass metabolism of the victim drugs in the gut was estimated using SimCYP and incorporated into the predictions. Because CYP3A4 is the major CYP enzyme in the gut wall, knowledge of the intrinsic gut clearance of a drug by this enzyme allows the prediction of net clearance by the gut (Thummel, et al., 1996). Exposure of enzymes to a drug during its transit through the gut wall also depends on uptake and efflux transporters, passive membrane permeability and enterocytic blood flow. All of these parameters are incorporated into the SimCYP simulation.

The in vivo degradation of CYP3A4 (k_{deg}) is a key input parameter for IVIVE of TDI-mediated DDIs. Since this is a physiological rather than drug-dependent parameter, it is often associated with uncertainty, with only indirect approaches available to estimate its value in humans. There are two approaches used to determine k_{deg}: in vitro liver models (liver slices and primary hepatocytes) and pharmacokinetically-based estimations (Ghanbari, et al., 2006). Additional uncertainty in the estimates of k_{deg} results from the assumptions that underlie the experimental models and the approaches used to analyze the results. Together, these uncertainties result in a relatively wide range of reported values. In the present study, a median of the reported values of k_{deg} (0.0144 hr^{-1} or $T_{1/2}$ = 48 hr) was chosen for the prediction by SimCYP (Yang, et al., 2008).

In the case of drugs whose metabolism is mediated by multiple isoforms of CYP (e.g., diazepam) the prediction of DDIs may be further complicated by possible dose-dependent changes in the contribution of each enzyme to overall metabolism (Rodrigues, 1999). The contribution of a given metabolic pathway to the total clearance of a drug is an important determinant of the accurate prediction of drug interactions. If the contribution of a pathway is small, its inhibition would not be predicted to have a significant effect on the AUC of the drug. To accurately measure the contribution of CYP3A4 to the metabolism of the drugs used in this study, SimCYP was used to incorporate kinetic capacities (K_m and V_{max}) of each individual CYP responsible for the metabolism of the drugs to ensure that the predicted DDIs were due solely to the inhibition of CYP3A4.

In conclusion, predictions of in vivo DDIs from in vitro TDI data (K_I and k_{inact}) measured in both HLM and hepatocytes were performed using SimCYP, a software simulator that incorporates a library of ADME information about the inhibitors and substrates, as well as information about genetic and physiological variability in the human population. The predicted DDIs from HLM and hepatocytes were correlated with clinically observed DDIs (n = 37). Based on the kinetic measurements, the magnitude of TDI in hepatocytes appeared to be generally weaker than that in HLM, suggesting that the intracellular concentrations of the inhibitors in the hepatocytes were lower than the nominal concentrations in the incubations. As a consequence, the magnitudes of clinical DDIs predicted from HLM were generally greater than those from hepatocytes and some predictions were substantially higher than clinically observed. Indeed, correlation analyses indicated a general trend of over-estimations in the DDI predictions from HLM. In contrast, one set of hepatocyte-based predictions (D1) showed close concordance between predicted and observed clinical DDIs, while the other (D2) under estimated the clinical DDIs. Collectively, these results show that hepatocytes could provide an alternative way to balance HLM-based predictions that can sometimes substantially over-estimate DDIs and possibly lead to erroneous conclusions about clinical risks.

Acknowledgement. We thank Dr. Masoud Jamei for providing comments on the model constructions in SimCyp for the DDI simulations.

Reference

Abernethy DR, Kaminsky LS and Dickinson TH (1991) Selective inhibition of warfarin metabolism by diltiazem in humans. *Journal of Pharmacology & Experimental Therapeutics* **257**:411-415.

Atkinson A, Kenny JR and Grime K (2005) Automated assessment of time-dependent inhibition of human cytochrome P450 enzymes using liquid chromatography-tandem mass spectrometry analysis. *Drug Metabolism & Disposition* **33**:1637-1647.

Austin RP, Barton P, Mohmed S and Riley RJ (2005) The binding of drugs to hepatocytes and its relationship to physicochemical properties.[see comment]. *Drug Metabolism & Disposition* **33**:419-425.

Backman JT, Olkkola KT, Aranko K, Himberg JJ and Neuvonen PJ (1994b) Dose of midazolam should be reduced during diltiazem and verapamil treatments. *British Journal of Clinical Pharmacology* **37**:221-225.

Bauer LA, Horn JR, Maxon MS, Easterling TR, Shen DD and Strandness DE, Jr. (2000) Effect of metoprolol and verapamil administered separately and concurrently after single doses on liver blood flow and drug disposition. *Journal of Clinical Pharmacology* **40**:533-543.

Calabresi L, Pazzucconi F, Ferrara S, Di PA, Tacca MD and Sirtori C (2004) Pharmacokinetic interactions between omeprazole/pantoprazole and clarithromycin in health volunteers. *Pharmacological Research* **49**:493-499.

Crivellato E, Candussio L, Rosati AM, Bartoli-Klugmann F, Mallardi F and Decorti G (2002) The fluorescent probe Bodipy-FL-Verapamil is a substrate for both P-glycoprotein and multidrug resistance-related protein (MRP)-1. *Journal of Histochemistry and Cytochemistry 50(5)()(pp 731-734), 2002 Date of Publication: 2002*731-734.

Einolf HJ (2007) Comparison of different approaches to predict metabolic drug-drug interactions. *Xenobiotica 37(10-11)()(pp 1257-1294), 2007 Date of Publication: Oct 2007*1257-1294.

Foti RS and Wahlstrom JL (2008) CYP2C19 inhibition: the impact of substrate probe selection on in vitro inhibition profiles. *Drug Metabolism & Disposition* **36**:523-528.

Freeman DJ, Martell R, Carruthers SG, Heinrichs D, Keown PA and Stiller CR (1987) Cyclosporin-erythromycin interaction in normal subjects. *British Journal of Clinical Pharmacology* **23**:776-778.

Furuta T, Ohashi K, Kobayashi K, Iida I, Yoshida H, Shirai N, Takashima M, Kosuge K, Hanai H, Chiba K, Ishizaki T and Kaneko E (1999) Effects of clarithromycin on the

metabolism of omeprazole in relation to CYP2C19 genotype status in humans. *Clinical Pharmacology & Therapeutics* **66**:265-274.

Genazzani E (1975) The pharmacological and pharmacokinetic properties of troleandomycin. *Quaderni di Antibiotica*35-56.

Ghanbari F, Rowland-Yeo K, Bloomer JC, Clarke SE, Lennard MS, Tucker GT and Rostami-Hodjegan A (2006) A critical evaluation of the experimental design of studies of mechanism based enzyme inhibition, with implications for in vitro-in vivo extrapolation. *Current Drug Metabolism 7(3)()(pp 315-334), 2006 Date of Publication: Apr 2006*315-334.

Gomez DY, Wacher VJ, Tomlanovich SJ, Hebert MF and Benet LZ (1995) The effects of ketoconazole on the intestinal metabolism and bioavailability of cyclosporine. *Clinical Pharmacology & Therapeutics* **58**:15-19.

Greenblatt DJ, von Moltke LL, Harmatz JS, Counihan M, Graf JA, Durol AL, Mertzanis P, Duan SX, Wright CE and Shader RI (1998a) Inhibition of triazolam clearance by macrolide antimicrobial agents: in vitro correlates and dynamic consequences. *Clinical Pharmacology & Therapeutics* **64**:278-285.

Greenblatt DJ, Wright CE, von Moltke LL, Harmatz JS, Ehrenberg BL, Harrel LM, Corbett K, Counihan M, Tobias S and Shader RI (1998c) Ketoconazole inhibition of triazolam and alprazolam clearance: differential kinetic and dynamic consequences. *Clinical Pharmacology & Therapeutics* **64**:237-247.

Guengerich FP (2003) Cytochromes P450, drugs, and diseases. [Review] [92 refs]. *Molecular Interventions* **3**:194-204.

Gupta SK, Bakran A, Johnson RW and Rowland M (1988) Erythromycin enhances the absorption of cyclosporin. *British Journal of Clinical Pharmacology* **25**:401-402.

Gurley B, Hubbard MA, Williams DK, Thaden J, Tong Y, Gentry WB, Breen P, Carrier DJ and Cheboyina S (2006) Assessing the clinical significance of botanical supplementation on human cytochrome P450 3A activity: comparison of a milk thistle and black cohosh product to rifampin and clarithromycin. *Journal of Clinical Pharmacology* **46**:201-213.

Gustavson LE, Kaiser JF, Edmonds AL, Locke CS, DeBartolo ML and Schneck DW (1995) Effect of omeprazole on concentrations of clarithromycin in plasma and gastric tissue at steady state. *Antimicrobial Agents & Chemotherapy* **39**:2078-2083.

He N, Huang SL, Zhu RH, Tan ZR, Liu J, Zhu B and Zhou HH (2003) Inhibitory effect of troleandomycin on the metabolism of omeprazole is CYP2C19 genotype-dependent. *Xenobiotica* **33**:211-221.

Hedaya MA, El-Afify DR and El-Maghraby GM (2006) The effect of ciprofloxacin and clarithromycin on sildenafil oral bioavailability in human volunteers. *Biopharmaceutics & Drug Disposition* **27**:103-110.

Hermann DJ, Krol TF, Dukes GE, Hussey EK, Danis M, Han YH, Powell JR and Hak LJ (1992) Comparison of verapamil, diltiazem, and labetalol on the bioavailability and metabolism of imipramine. *Journal of Clinical Pharmacology* **32**:176-183.

Ito K, Iwatsubo T, Kanamitsu S, Ueda K, Suzuki H and Sugiyama Y (1998) Prediction of pharmacokinetic alterations caused by drug-drug interactions: metabolic interaction in the liver. [Review] [93 refs]. *Pharmacological Reviews* **50**:387-412.

Ito K, Ogihara K, Kanamitsu S and Itoh T (2003) Prediction of the in vivo interaction between midazolam and macrolides based on in vitro studies using human liver microsomes. *Drug Metabolism & Disposition* **31**:945-954.

Jacobson TA (2004b) Comparative pharmacokinetic interaction profiles of pravastatin, simvastatin, and atorvastatin when coadministered with cytochrome P450 inhibitors. *American Journal of Cardiology* **94**:1140-1146.

Jayasagar G, Dixit AA, Kishan V and Rao YM (2000) Effect of clarithromycin on the pharmacokinetics of tolbutamide. *Drug Metabolism & Drug Interactions* **16**:207-215.

Kantola T, Kivisto KT and Neuvonen PJ (1998a) Erythromycin and verapamil considerably increase serum simvastatin and simvastatin acid concentrations.[see comment]. *Clinical Pharmacology & Therapeutics* **64**:177-182.

Kharasch ED, Hoffer C, Whittington D and Sheffels P (2004) Role of hepatic and intestinal cytochrome P450 3A and 2B6 in the metabolism, disposition, and miotic effects of methadone. *Clinical Pharmacology & Therapeutics* **76**:250-269.

Kim M, Shen DD, Eddy AC and Nelson WL (1993) Inhibition of the enantioselective oxidative metabolism of metoprolol by verapamil in human liver microsomes. *Drug Metabolism and Disposition 21(2)()(pp 309-317), 1993 Date of Publication: 1993*309-317.

Matic S, Geisler DA, Moller IM, Widell S and Rasmusson AG (2005) Alamethicin permeabilizes the plasma membrane and mitochondria but not the tonoplast in tobacco (Nicotiana tabacum L. cv Bright Yellow) suspension cells. *Biochemical Journal* **389**:3-704.

Mayhew BS, Jones DR and Hall SD (2000) An in vitro model for predicting in vivo inhibition of cytochrome P450 3A4 by metabolic intermediate complex formation. *Drug Metabolism & Disposition* **28**:1031-1037.

McConn DJ, Lin YS, Allen K, Kunze KL and Thummel KE (2004) Differences in the inhibition of cytochromes P450 3A4 and 3A5 by metabolite-inhibitor complex-forming drugs. *Drug Metabolism & Disposition* **32**:1083-1091.

McLean AJ, Knight R, Harrison PM and Harper RW (1985) Clearance-based oral drug interaction between verapamil and metoprolol and comparison with atenolol. *American Journal of Cardiology* **55**:t-9.

Muirhead GJ, Faulkner S, Harness JA and Taubel J (2002) The effects of steady-state erythromycin and azithromycin on the pharmacokinetics of sildenafil in healthy volunteers. *British Journal of Clinical Pharmacology* **53**:Suppl-43S.

Murdoch DL, Thomson GD, Thompson GG, Murray GD, Brodie MJ and McInnes GT (1991) Evaluation of potential pharmacodynamic and pharmacokinetic interactions between verapamil and propranolol in normal subjects. *British Journal of Clinical Pharmacology* **31**:323-332.

Obach RS, Walsky RL and Venkatakrishnan K (2007) Mechanism-based inactivation of human cytochrome p450 enzymes and the prediction of drug-drug interactions. *Drug Metabolism & Disposition* **35**:246-255.

Obach RS, Walsky RL, Venkatakrishnan K, Houston JB and Tremaine LM (2005) In vitro cytochrome P450 inhibition data and the prediction of drug-drug interactions: qualitative relationships, quantitative predictions, and the rank-order approach. [Review] [43 refs]. *Clinical Pharmacology & Therapeutics* **78**:582-592.

Olkkola KT, Aranko K, Luurila H, Hiller A, Saarnivaara L, Himberg JJ and Neuvonen PJ (1993) A potentially hazardous interaction between erythromycin and midazolam. *Clinical Pharmacology & Therapeutics* **53**:298-305.

Phillips JP, Antal EJ and Smith RB (1986) A pharmacokinetic drug interaction between erythromycin and triazolam. *Journal of Clinical Psychopharmacology* **6**:297-299.

Phimmasone S and Kharasch ED (2001) A pilot evaluation of alfentanil-induced miosis as a noninvasive probe for hepatic cytochrome P450 3A4 (CYP3A4) activity in humans. *Clinical Pharmacology & Therapeutics* **70**:505-517.

Polasek TM, Elliot DJ, Lewis BC and Miners JO (2004) Mechanism-based inactivation of human cytochrome P4502C8 by drugs in vitro. *Journal of Pharmacology & Experimental Therapeutics* **311**:996-1007.

Rodrigues AD (1999) Integrated cytochrome P450 reaction phenotyping: attempting to bridge the gap between cDNA-expressed cytochromes P450 and native human liver microsomes. [Review] [49 refs]. *Biochemical Pharmacology* **57**:465-480.

Rodrigues AD, Roberts EM, Mulford DJ, Yao Y and Quellet D (1997) Oxidative metabolism of clarithromycin in the presence of human liver microsomes: Major role for the cytochrome P4503A (CYP3A) subfamily. *Drug Metabolism and Disposition 25(5)()(pp 623-630), 1997 Date of Publication: May 1997*623-630.

Rodvold KA (1999) Clinical pharmacokinetics of clarithromycin. [Review] [110 refs]. *Clinical Pharmacokinetics* **37**:385-398.

Rostami-Hodjegan A and Tucker GT (2007) Simulation and prediction of in vivo drug metabolism in human populations from in vitro data. [Review] [64 refs]. *Nature Reviews* **Drug**:140-148.

Saeki T, Ueda K, Tanigawara Y, Hori R and Komano T (1993) P-glycoprotein-mediated transcellular transport of MDR-reversing agents. *FEBS Letters 324(1)()(pp 99-102), 1993 Date of Publication: 1993*99-102.

Sirmans SM, Pieper JA, Lalonde RL, Smith DG and Self TH (1988) Effect of calcium channel blockers on theophylline disposition. *Clinical Pharmacology & Therapeutics* **44**:29-34.

Sketris IS, Wright MR and West ML (1996) Possible role of the intestinal P-450 enzyme system in a cyclosporine-clarithromycin interaction. *Pharmacotherapy* **16**:301-305.

Sutton D, Butler AM, Nadin L and Murray M (1997) Role of CYP3A4 in human hepatic diltiazem N-demethylation: Inhibition of CYP3A4 activity by oxidized diltiazem metabolites. *Journal of Pharmacology and Experimental Therapeutics 282(1)()(pp 294-300), 1997 Date of Publication: Jul 1997*294-300.

Takano M, Hasegawa R, Fukuda T, Yumoto R, Nagai J and Murakami T (1998) Interaction with P-glycoprotein and transport of erythromycin, midazolam and ketoconazole in Caco-2 cells. *European Journal of Pharmacology 358(3)()(pp 289-294), 1998 Date of Publication: 09 Oct 1998*289-294.

Thummel KE, O'Shea D, Paine MF, Shen DD, Kunze KL, Perkins JD and Wilkinson GR (1996) Oral first-pass elimination of midazolam involves both gastrointestinal and hepatic CYP3A-mediated metabolism. *Clinical Pharmacology & Therapeutics* **59**:491-502.

Tracy TS, Korzekwa KR, Gonzalez FJ and Wainer IW (1999) Cytochrome P450 isoforms involved in metabolism of the enantiomers of verapamil and norverapamil. *British Journal of Clinical Pharmacology 47(5)()(pp 545-552), 1999 Date of Publication: 1999*545-552.

von Moltke LL, Greenblatt DJ, Schmider J, Wright CE, Harmatz JS and Shader RI (1998) In vitro approaches to predicting drug interactions in vivo. [Review] [107 refs]. *Biochemical Pharmacology* **55**:113-122.

Wadhwa NK, Schroeder TJ, O'Flaherty E, Pesce AJ, Myre SA, Munda R and First MR (1987) Interaction between erythromycin and cyclosporine in a kidney and pancreas allograft recipient. *Therapeutic Drug Monitoring* **9**:123-125.

Wang JS, Wang W, Xie HG, Huang SL and Zhou HH (1997a) Effect of troleandomycin on the pharmacokinetics of imipramine in Chinese: the role of CYP3A. *British Journal of Clinical Pharmacology* **44**:195-198.

Wang RW, Newton DJ, Scheri TD and Lu AYH (1997b) Human cytochrome P450 3A4-catalyzed testosterone 6beta-hydroxylation and erythromycln N-demethylation: Competition during catalysis. *Drug Metabolism and Disposition 25(4)()(pp 502-507), 1997 Date of Publication: Apr 1997*502-507.

Warot D, Bergougnan L, Lamiable D, Berlin I, Bensimon G, Danjou P and Puech AJ (1987) Troleandomycin-triazolam interaction in healthy volunteers: pharmacokinetic and psychometric evaluation. *European Journal of Clinical Pharmacology* **32**:389-393.

Wester MR, Lasker JM, Johnson EF and Raucy JL (2000) CYP2C19 participates in tolbutamide hydroxylation by human liver microsomes. *Drug Metabolism & Disposition* **28**:354-359.

Yang J, Jamei M, Heydari A, Yeo KR, de la TR, Farre M, Tucker GT and Rostami-Hodjegan A (2006) Implications of mechanism-based inhibition of CYP2D6 for the pharmacokinetics and toxicity of MDMA. *Journal of Psychopharmacology* **20**:842-849.

Yang J, Jamei M, Yeo KR, Tucker GT and Rostami-Hodjegan A (2007) Prediction of intestinal first-pass drug metabolism. [Review] [149 refs]. *Current Drug Metabolism* **8**:676-684.

Yang J, Liao M, Shou M, Jamei M, Yeo KR, Tucker GT and Rostami-Hodjegan A (2008) Cytochrome p450 turnover: regulation of synthesis and degradation, methods for determining rates, and implications for the prediction of drug interactions. [Review] [146 refs]. *Current Drug Metabolism* **9**:384-394.

Yasui N, Otani K, Kaneko S, Ohkubo T, Osanai T, Sugawara K, Chiba K and Ishizaki T (1996) A kinetic and dynamic study of oral alprazolam with and without erythromycin in humans: in vivo evidence for the involvement of CYP3A4 in alprazolam metabolism. *Clinical Pharmacology & Therapeutics* **59**:514-519.

Yeates RA, Laufen H and Zimmermann T (1996) Interaction between midazolam and clarithromycin: comparison with azithromycin. *International Journal of Clinical Pharmacology & Therapeutics* **34**:400-405.

Yeo KR and Yeo WW (2001) Inhibitory effects of verapamil and diltiazem on simvastatin metabolism in human liver microsomes. *British Journal of Clinical Pharmacology* **51**:461-470.

Zimmermann T, Yeates RA, Laufen H, Scharpf F, Leitold M and Wildfeuer A (1996) Influence of the antibiotics erythromycin and azithromycin on the pharmacokinetics and pharmacodynamics of midazolam. *Arzneimittel-Forschung* **46**:213-217.

Footnotes.

Send the reprint requests to:

Magang Shou, Ph.D.
Department of Pharmacokinetics and Drug Metabolism
30E-2-B, Amgen, Inc.
One Amgen Center Drive
Thousand Oaks, CA91320-1799
Tel: (805) 447-4247
Fax: (805) 375-9515
E-mail: mshou@amgen.com

Legends for figures

Figure 1. Remaining of MDZ (%) and formation of 1-OH MDZ (peak area ratio of metabolite to internal standard) as a function of incubation time (up to 30 min) in human hepatocytes (10^6 cells/mL).

Figure 2. Fitting curves of observed k_{obs} versus inhibitor concentration by non-linear regression analyses with Eqn. 2. Observed k_{obs} values are the slopes obtained from the linear regression of % enzyme activity remaining (Ln scale) versus preincubation time of each inhibitor at varying concentrations. The fitting curves of the five inhibitors are obtained from HLM (**A**); hepatocyte donor 1 (**B**); and hepatocyte donor 2 (**C**), respectively.

Figure 3. An example of SimCYP simulations of human pharmacokinetic DDIs predicted from in vitro TDI data in HLM or hepatocytes: (**A**) mean values of systemic CLA concentration in plasma over time (dose regimen in Table 2: 500 mg, Bid, 9 days); (**B**) mean values of systemic simvastatin concentration in plasma over time (40 mg) in the presence and absence of CLA (AUC ratio, ± CLA = 6.7); (**C**) mean values of hepatic CYP3A4 CL_{int} over time (± CLA) and (**D**) mean values of gut CYP3A4 CL_{int} over time (± CLA).

Figure 4. Correlation analyses of in vivo DDIs predicted from in vitro TDI in HLM and hepatocytes. LR, linear regression; 95% CI, 95% confidence interval; 95% PI, 95% prediction interval. (**A**) Correlation of predicted DDIs from TDI data between HLM and hepatocytes (D1); (**B**) between HLM and hepatocytes (D2); and (**C**) between the two hepatocyte donors (D1 and D2).

Figure 5. Correlation analyses of predicted DDIs from in vitro TDI in (**A**) HLM, (**C**) hepatocyte donor 1 (D1) and (**E**) hepatocyte donor 2 (D2) to observed in vivo DDIs. Observed DDIs within a 2-fold range of model-predicted values from (**B**) HLM, (**D**) hepatocyte donor 1 (D1) and (**F**) hepatocyte donor 2 (D2). LR, linear regression; 95% CI, 95% confidence interval; 95% PI, 95% prediction interval.

Table 1. Unbound fractions of the five inhibitors in human plasma, liver microsomes and hepatocytes.

Drug	$f_{u,p}$ (plasma)	$f_{u,mics}$ (HLM)	$f_{u,hept}$ (hepatocytes)		
			No treatment	Alamethicin	ABT
CLA	0.175	0.324	0.806	0.980	0.750
DIL	0.212	0.820	0.709	0.890	0.788
ERY	0.326	0.870	0.465	0.936	0.918
VER	0.069	0.587	0.883	0.936	0.877
TAO	0.015	0.154	0.567	0.715	0.692

Table 2. $f_{m, CYP3A4}$ of the substrates (n = 100 individuals) used in SimCyp for simulation of DDIs.

	$f_{m,CYP3A4}$ (%)	
	Mean (SD)	Median (5^{th} -95^{th} %)
Alprazolam	91.3 (14.0)	100 (63.9 – 100)
Cyclosporine	90.8 (21.0)	100 (35.0-100)
Imipramine	2.0 (1.7)	1.5 (0.1-3.8)
Metoprolol	14.7 (24.7)	6.7 (1.2-100)
Midazolam	83.7 (29.8)	100 (20.0-100)
Omeprazole	24.3 (20.6)	17.6 (4.2-60.7)
Sildenafil	82.3 (13.0)	87.0 (67.7-96.5)
Simvastatin	83.4 (11.7)	86.9 (58.0-97.1)
Theophylline	1.8 (1.3)	2.1 (0-5.0)
Tolbutamide	2.1 (1.2)	1.6 (0-4.8)
Triazolam	85.7 (26.4)	100 (27.2-100)

Table 3. Pharmacokinetic parameters of the inhibitors used for DDI simulations.

Inhibitor	K_a (h^{-1})	$V_{d, ss}$ (L/kg)	CL_{PO} (L/h)	Dose regimen	Simulated $[I]_{max, ss}$ (ug/mL)	Observed $[I]_{max, ss}$ (ug/mL)	References
DIL	1.69	3.09	175.8	120 mg Tid 13d	0.15	0.18	(Abernethy, et al., 1991)
CLA[a]	1.7	2.0	58.1	500 mg Bid 7d	1.07	2.27	(Calabresi, et al., 2004)
ERY	0.26	1.27	63.6	500 mg Tid 7d	1.2	1.2	(Olkkola, et al., 1993)
VER	1.22	3.40	85.4	120 mg Tid 7d	0.15	0.25	(Murdoch, et al., 1991)
TAO[a]	0.46	2.14	30.0	500 mg Sd	1.08	1.77	(Genazzani, 1975)

[a.] The PK parameters for CLA and TAO were obtained, respectively from Rodvold et al. (Rodvold, 1999) and Genazzani et al. (Genazzani, 1975) and incorporated into SimCYP for PK simulation.

Table 4. Kinetic parameters of the five inhibitors for the time dependent CYP3A4 inhibition from human pooled liver microsomes and hepatocytes from two donors.

Inhibitor	Conc. range (μM)	Hepatocytes						HLM		
		Donor 1			Donor 2					
		K_I (μM)[a]	$K_{I,u}$ (μM)[b]	k_{inact} (min^{-1})[a]	K_I (μM)	$K_{I,u}$ (μM)	k_{inact} (min^{-1})	K_I (μM)[c]	$K_{I,u}$ (μM)	k_{inact} (min^{-1})
CLA	12.8-80	7.88 (3.09)	7.64	0.040 (0.005)	17.20 (2.80)	16.86	0.028 (0.002)	15.72 (3.52)	5.09	0.063 (0.008)
DIL	0.25-16	3.55 (1.33)	3.12	0.027 (0.004)	3.80 (0.59)	3.38	0.014 (0.001)	0.67 (0.2)	0.55	0.019 (0.014)
ERY	0.5-500	21.40 (4.60)	20.03	0.016 (0.002)	116.0 (6.10)	108.58	0.055 (0.001)	1.70 (0.49)	1.48	0.017 (0.002)
VER	0.31-20	2.99 (0.35)	2.80	0.032 (0.001)	2.58 (0.57)	2.41	0.020 (0.001)	3.50 (1.47)	2.05	0.053 (0.007)
TAO	0.05-1.6	0.56 (0.084)	0.40	0.050 (0.004)	1.05 (0.11)	0.75	0.038 (0.002)	0.19 (0.04)	0.03	0.065 (0.004)

[a.] K_I and k_{inact} of each inhibitor in hepatocytes and HLM (SD in parenthesis) were obtained from non-linear regression analyses of observed k_{obs} values shown in Figure 2. Values in parenthesis present standard deviations. [b.] $K_{I,u}$ values were calculated by K_I multiplied by f_u shown in Table 2. c. In addition to the K_I values measured in the study, they were also reported in literature: CLA = 5.49 μM, 0.072 min^{-1} (Mayhew, et al., 2000); DIL = 3.3 μM, 0.07 min^{-1} (Yeo and Yeo, 2001); ERY = 10.9 μM, 0.046 min^{-1} (McConn, et al., 2004); VER= 2.9 μM, 0.15 min^{-1} (Yeo and Yeo, 2001); VER = 4.2 μM, 0.092 min^{-1} (Polasek, et al., 2004) and TAO= 0.26 μM, 0.12 min^{-1} (Atkinson, et al., 2005).

Table 5. Predictions of human DDIs from in vitro TDI of CYP3A4 using SimCYP simulator.

Inhibitor	Inhibitor Dose Regimen[a]	Simulated $[I]_{max,ss}$ (μg/mL)[b]	Substrate	Substrate Dose Regimen[c]	PRED[d] (D1)	PRED[d] (D2)	PRED[e] (HLM)	OBS[f]	Reference
ERY	400 mg Tid 10d	0.96	alprazolam	0.8 mg	1.89 (1.2-9.4)	1.52 (1.1-2.5)	1.73 (1.2-16.8)	2.47	(Yasui, et al., 1996)
	500 mg Qid 3d	2.03	cyclosporine	350 mg	3.15 (1.5-15.5)	2.05 (1.3-3.4)	3.30 (1.6-21.4)	2.14	(Gupta, et al., 1988)
	250 mg Qid 7d	0.73	cyclosporine	700 mg	2.44 (1.5-5.2)	1.59 (1.2-2.5)	2.69 (1.4-12.9)	2.22	(Freeman, et al., 1987)
	250 mg Qid 3d	0.73	cyclosporine	150 mg	3.18 (1.8-7.6)	1.53 (1.2-2.1)	3.67 (1.6-17.3)	1.7	(Wadhwa, et al., 1987)
	500 mg Tid 5d	1.20	midazolam	15 mg	6.1 (3.3-22.1)	3.02 (1.7-5.3)	14.10 (2.1-65.4)	3.81	(Zimmermann, et al., 1996)
	500 mg Tid 7d	1.20	midazolam	15 mg	6.1 (3.3-22.1)	3.42 (1.8-5.7)	14.5 (2.2-59.3)	4.41	(Olkkola, et al., 1993)
	500 mg Bid 5d	0.97	sildenafil	100 mg	4.65 (2.4-10.8)	2.02 (1.4-3.0)	5.81 (2.0-27.4)	2.83	(Muirhead, et al., 2002)
	500 mg Tid 2d	1.20	simvastatin	40 mg	7.56 (5.9-18.9)	4.28 (2.7-5.3)	18.2 (5.6-45.8)	6.21	(Kantola, et al., 1998a)
	333 mg Tid 3d	0.80	triazolam	0.5 mg	4.47 (2.3-11.5)	1.52 (1.2-1.9)	5.61 (2.1-37.4)	2.06	(Phillips, et al., 1986)
	500 mg Bid 2d	0.98	triazolam	0.125 mg	4.33 (2.3-11.2)	1.29 (1.1-1.5)	5.62 (2.1-36.8)	3.8	(Greenblatt, et al., 1998a)
VER	80 mg Qd 2d	0.069	metoprolol	50 mg	1.04 (1.0-1.2)	1.00 (1.0-1.0)	1.02 (1.0-1.7)	1.33	(Bauer, et al., 2000)
	120 mg Tid 7d	0.15	imipramine	100 mg	1.01 (1.0-1.1)	1.01 (1.0-1.0)	1.01 ((1.0-1.1)	1.15	(Hermann, et al., 1992)
	120 mg Tid 7d	0.15	metoprolol	100 mg	1.16 (1.0-1.8)	1.03 (1.0-1.1)	1.13 (1.0-1.9)	1.79	(McLean, et al., 1985)

	80 mg Tid 2d	0.1	midazolam	15 mg	2.14 (1.3-4.7)	1.32 (1.1-1.7)	3.71 (1.6-12.5)	2.91	(Backman, et al., 1994a)
	480 mg Qd 3d	0.427	simvastatin	40 mg	4.19 (1.9-15.7)	3.58 (1.7-7.2)	6.89 (1.7-23.1)	4.21	(Jacobson, 2004b)
	80 mg Tid 2d	0.1	simvastatin	40 mg	2.59 (1.8-4.3)	1.62 (1.2-2.2)	4.35 (2.0-15.4)	4.65	(Kantola, et al., 1998b)
	120 mg Tid 7d	0.15	theophylline	5 mg/kg	1.00 (1.0-1.0)	1.00 (1.0-1.0)	1.00 (1.0-1.1)	1.24	(Sirmans, et al., 1988)
CLA	500 mg Bid 8d	1.07	cyclosporine	75 mg	2.81 (1.5-8.8)	2.11 (1.3-3.5)	3.46 (1.7-11.9)	1.98	(Sketris, et al., 1996)
	250 mg Bid 5d	0.534	midazolam	15 mg	3.94 (1.6-14.5)	2.12 (1.2-4.1)	2.69 (1.8-17.9)	3.57	(Yeates, et al., 1996)
	500 mg Bid 7d	1.07	midazolam	8 mg	5.6 (1.9-22.5)	4.03 (1.4-8.8)	7.9 (2.1-33.3)	8.39	(Gurley, et al., 2006)
	500 mg Bid 7d	1.07	omeprazole	20 mg	1.9 (1.1-6.7)	1.25 (1.1-1.6)	2.1 (1.2-10.7)	2.01	(Calabresi, et al., 2004)
	400 mg Bid 3d	0.86	omeprazole	20 mg	1.93 (1.2-6.7)	1.17 (1.0-1.5)	2.19 (1.2-10.7)	2.10	(Furuta, et al., 1999)
	400 mg Bid 3d	0.86	omeprazole	20 mg	1.93 (1.2-6.7)	1.17 (1.0-1.5)	2.19 (1.2-10.7)	2.11	(Furuta, et al., 1999)
	400 mg Bid 3d	0.86	omeprazole	20 mg	1.93 (1.2-6.7)	1.17 (1.0-1.5)	2.19 (1.2-10.7)	2.34	(Furuta, et al., 1999)
	500 mg Tid 5d	1.29	omeprazole	40 mg	2.23 (1.2-11.7)	1.31 (1.1-1.8)	2.47 (1.2-19.5)	1.91	(Gustavson, et al., 1995)
	500 mg Sd	0.95	sildenafil	50 mg	1.03 (1.0-1.1)	1.07 (1.0-1.1)	1.02 (1.0-1.1)	2.28	(Hedaya, et al., 2006)
	500 mg Bid 9d	1.29	simvastatin	40 mg	6.7 (4.1-18.1)	5.79 (1.9-11.8)	11.2 (3.7-40.4)	9.95	(Jacobson, 2004a)
	250 mg Sd	0.47	tolbutamide	500 mg	1.00 (1.0-1.1)	1.00 (1.0-1.0)	1.00 (1.0-1.0)	1.25	(Jayasagar, et al., 2000)
	500 mg Bid 2d	1.07	triazolam	0.125 mg	3.15 (2.0-7.2)	1.67 (1.1-2.6)	3.9 (1.8-13.1)	5.25	(Greenblatt, et al., 1998b)
DIL	60 mg Tid 2d	0.037	midazolam	15 mg	2.55	1.31	5.4	3.75	(Backman, et al., 1994b)

					(1.6-4.8)	(1.2-1.6)	(2.0-21.2)		
TAO	250 mg Qd 2d	0.48	imipramine	100 mg	1.01 (1.0-1.1)	1.01 (1.0-1.0)	1.01 (1.0-1.1)	1.59	(Wang, et al., 1997a)
	500 mg Sd	1.08	midazolam	1 mg	5.02 (2.2-9.4)	2.51 (1.8-5.1)	13.7 (2.3-30.6)	4.39	(Kharasch, et al., 2004)
	500 mg Sd	1.08	midazolam	3 mg	5.02 (2.2-9.4)	2.51 (1.8-5.1)	13.7 (1.9-20.6)	4.64	(Phimmasone and Kharasch, 2001)
	500 mg Qd 2d	0.96	omeprazole	20 mg	2.18 (1.3-3.3)	1.30 (1.1-1.7)	2.57 (1.2-16.6)	1.26	(He, et al., 2003)
	500 mg Qd 2d	0.96	omeprazole	20 mg	2.18 (1.3-3.3)	1.30 (1.1-1.7)	2.57 (1.2-26.6)	1.28	(He, et al., 2003)
	500 mg Qd 2d	0.96	omeprazole	20 mg	2.18 (1.3-3.3)	1.30 (1.1-1.7)	2.57 (1.2-26.6)	1.81	(He, et al., 2003)
	1000mg Bid 7d	2.15	triazolam	0.25 mg	4.21 (2.3-12.0)	3.40 (2.1-5.8)	5.65 (2.9-15.5)	3.75	(Warot, et al., 1987)

[a.] Inhibitor dose regimen, for example, 500 mg Tid 5d represents the inhibitor dosed at 500 mg, three time a day for 5 consecutive days; [b.] $[I]_{max,ss}$ = simulated maximum inhibitor plasma concentrations at steady state; [c.] Victim drug dose regimen (single dose); [d.] Predicted DDIs (median of total population) from in vitro TDI measured in hepatocytes from donors 1 (D1) and 2 (D2), respectively, and the values in parenthesis represent minimum (5^{th}%) and maximum (95^{th}%) DDI values obtained from the 10 individual trials; [e.] Predicted DDIs (median of total population) from in vitro TDI measured in HLM and the values in parenthesis represent minimum and maximum DDI values obtained from the 10 trials; and [f.] Clinically observed DDIs calculated by AUC in the presence and absence of inhibitor.

Figure 1

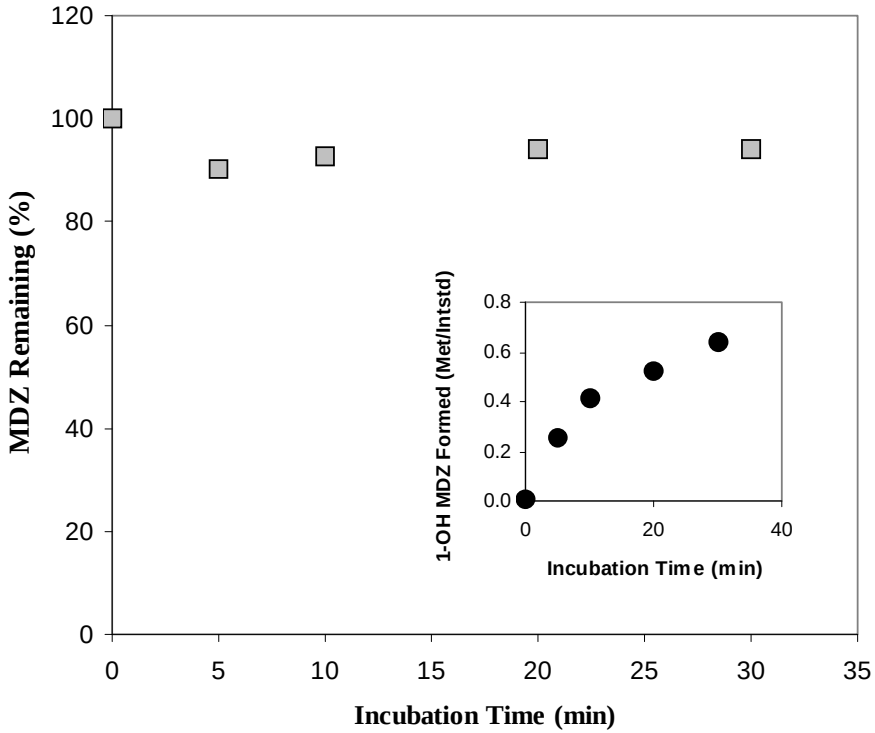

Figure 2

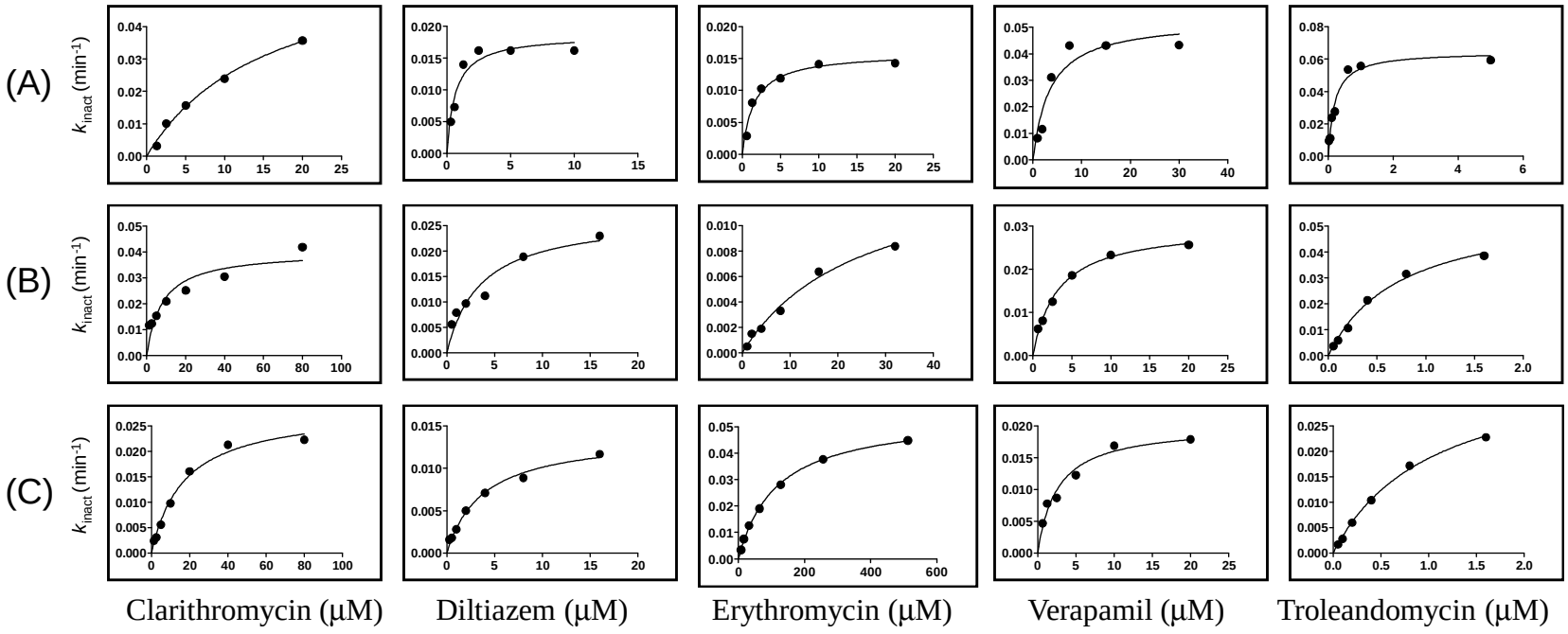

Figure 3

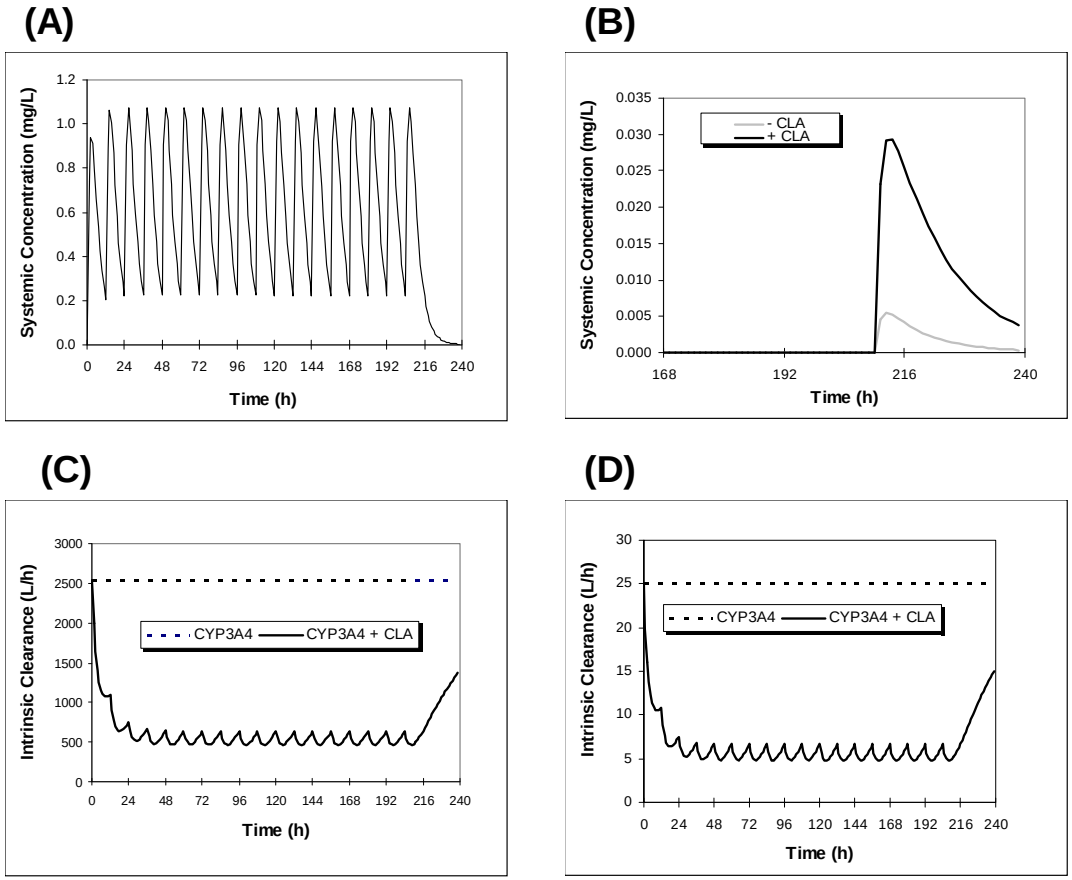

DMD Fast Forward. Published on September 22, 2009 as DOI: 10.1124/dmd.108.025494
This article has not been copyedited and formatted. The final version may differ from this version.

Figure 4

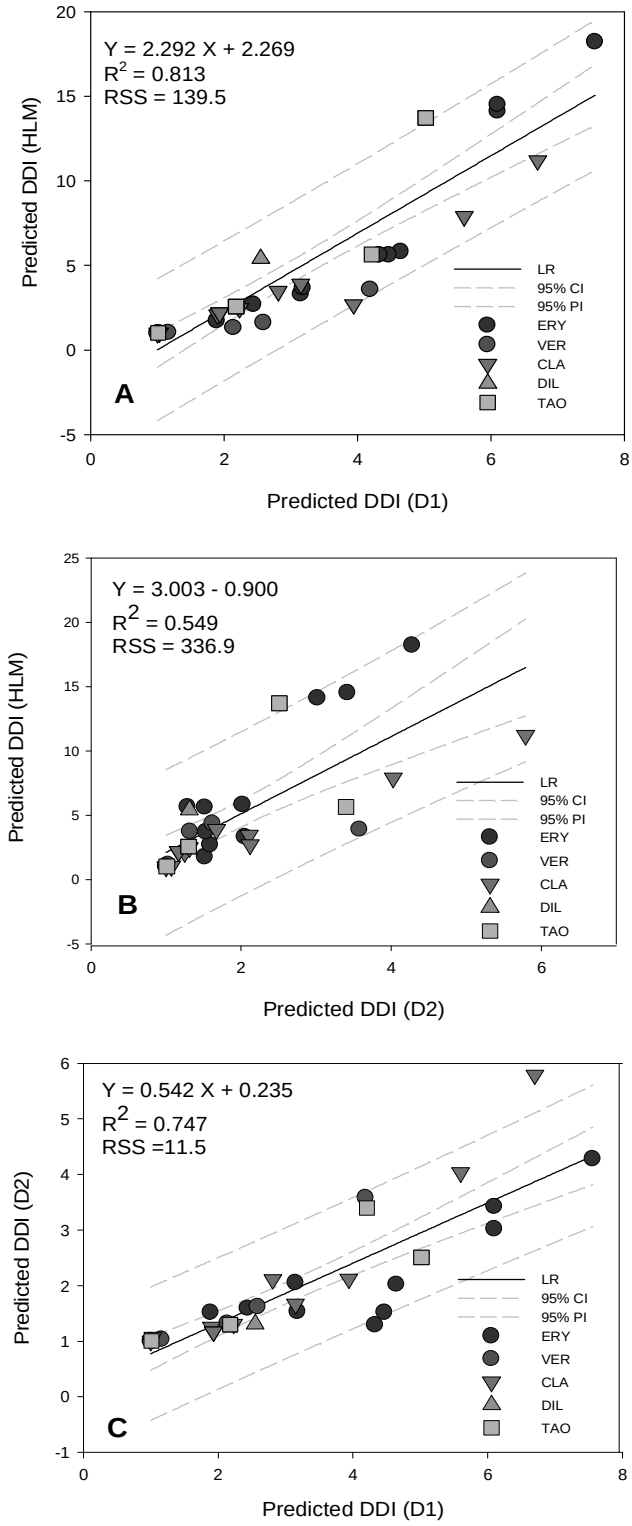

DMD Fast Forward. Published on September 22, 2009 as DOI: 10.1124/dmd.108.025494
This article has not been copyedited and formatted. The final version may differ from this version.

Figure 5